Materials Science Forum Vols. 449-452 (2004) pp. 849-852
online at http://www.scientific.net

Fatigue and Contact Damage of Layered Machinable Ti_3SiC_2 Ceramics

Z.G. Wang[1†], H. Zhang[1], Q.S. Zang[1], Z.F. Zhang[2] and Z.M. Sun[2]

[1] Materials Fatigue and Fracture Division, Shenyang Laboratory for Materials Science, Institute of Metal Research, Chinese Academy of Sciences, Wenhua road 72, Shenyang 110016, P. R. China
[2] AIST Tohoku, National Institute of Advanced Industrial Science and Technology, 4-2-1, Nigatake, Miyagino-ku, Sendai 983-8551, Japan

Keywords: Ti_3SiC_2; Fatigue; Microstructure; Hertzian contact; Strength degradation

1. Introduction

Ti_3SiC_2 has been widely investigated for their intriguing physical and mechanical properties [1]. In the past decades, dense and pure polycrystalline Ti_3SiC_2 has been fabricated by some techniques [1,2]. Studies on deformation and fracture behavior at elevated temperature showed that Ti_3SiC_2 exhibited substantial plasticity with high strength [3]. It is pointed out that Ti_3SiC_2 can be possibly used for some contact applications, such as bearings, for its relative high compression strength, self-lubricating and machinability [1]. In the present paper, fatigue crack-growth rates and Hertzian contact damage of Ti_3SiC_2 were studied. Shielding ability of Ti_3SiC_2 was investigated specially in the small crack region. Damage evolution and strength degradation under Hertzian contact were studied to reveal damage behavior and mechanisms in Ti_3SiC_2.

2. Experimental Procedures

2.1 Material and Microstructure

The synthesis process of Ti_3SiC_2 was conducted at 1200~1400 ℃ with pulse discharge sintering (PDS) technique [2]. Heterogeneous microstructure of Ti_3SiC_2 in this study consists of elongated and equiaxed grain. The elongated grain was typically ~50 μm long and ~15 μm wide, while the average size of equiaxed grain was ~5 μm. Characteristic microstructures are shown in Fig. 1.

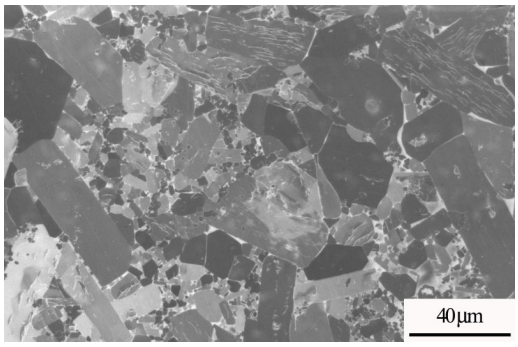

Fig. 1 Optical micrograph of pulse discharge sintered Ti_3SiC_2

2.2 Cyclic fatigue crack-growth rates

Cyclic fatigue tests were performed using compact-tension (CT) specimens (2.6 mm thick). Specimens were cycled at a frequency of 20 Hz (sine wave) under load control at a load ratio R of 0.1 and 0.5. Tests began at an applied maximum cyclic load of 300 N. Load was increased by 10 N every 10^5 cycles until a fatigue pre-crack was initiated from a straight-through notch. Cracks were always found to decelerate first and to be arrested finally with the number of cycles. The load was then increased to restart the crack until the crack length increased steadily with the number of cycles.

Corresponding author : zhgwang@imr.ac.cn

Crack growth rates were controlled under load-decreasing conditions to approach to the fatigue threshold stress intensity range, ΔK_{th}. An experiment at constant K_{max} with decreasing-K_{min} (R is variable) was performed in order to elucidate the contribution of ΔK and K_{max} to the crack growth rate and corresponding mechanisms.

2.3 Cyclic Fatigue under Hertzian contact

Bonded-interface [4] and three-points bending specimen were employed to investigate contact fatigue of Ti_3SiC_2. Repeat indentations were made on the polished surface of the specimen symmetrically across the interface trace with a sphere of radius 2.95 mm using a Shimadzu servo-hydraulic material testing machine. A load range 0~1000 N was applied at a frequency of 10 Hz (sinusoidal wave), up to 10^6 cycles.

Bar specimen configuration was used for strength degradation tests. Cyclic load was applied on the polished surfaces of three-point bending specimen using a GCr15 sphere indenter of radius r = 2.95 mm at a frequency of 10 Hz. Flexural strength was obtained by fracturing the indented bar specimen at a speed of 0.5 mm/min.

3. Results and Discussions

3.1 Cyclic fatigue crack-growth rates

A. Small crack behavior

Cyclic fatigue crack length versus number of cycles at different load amplitudes after pre-cracking is shown in Fig. 2. Cracks were often observed to propagate and arrest completely during the first applied ~10^5 cycles until a higher load amplitude is applied. This is presumably caused by the principal role of crack bridging by single or clusters of grain in the wake of crack tip. Such bridging zone may produce shielding stress intensity, K_{sh}. It is assumed that the applied stress intensity, K_{appl} must exceed the sum of the intrinsic toughness, K_0, and K_{sh}, i.e.

$$K_{appl} \geq K_0 + K_{sh}$$

in order for a crack to propagate. Here K_{sh} generally increases during crack propagation if the shielding bridging zone is not fully evolved. Therefore it is presumed that the shielding stress intensity, K_{sh}, increases with the crack length faster than the applied stress intensity, K_{appl}, and this results in a decrease in the stress intensity experienced at the crack tip, and therefore in a reduced crack growth rate.

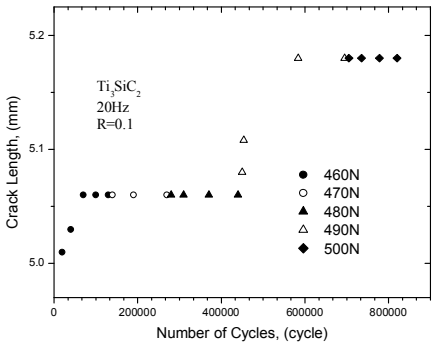

Fig. 2 Small crack behavior of Ti_3SiC_2

B. Characteristics of fatigue crack growth rate

Fatigue crack growth rates, da/dN, plotted as functions of the applied stress intensity range, ΔK, and the applied maximum stress intensity, K_{max}, are shown in Fig. 3. Crack growth rates are accelerated and the thresholds ΔK_{th} reduced with increasing R at a fixed ΔK, whereas, in

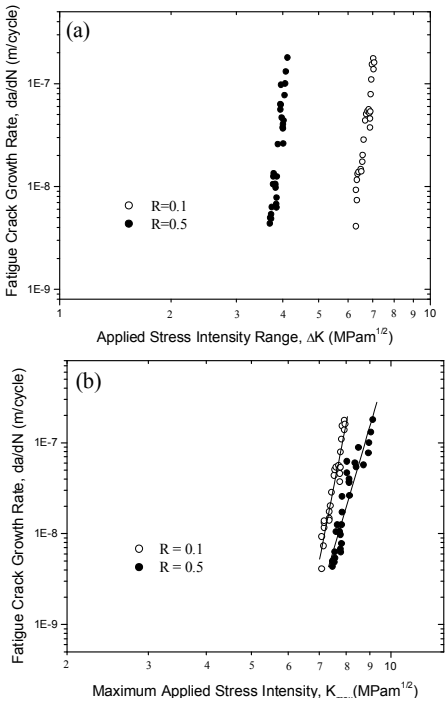

Fig. 3 Relationship between crack growth rates da/dN and (a) the applied stress intensity range ΔK, (b) the applied maximum stress intensity K_{max} at load ratios, R, of 0.1 and 0.5.

Fig. 3(b), the influence of R on the crack growth rate is

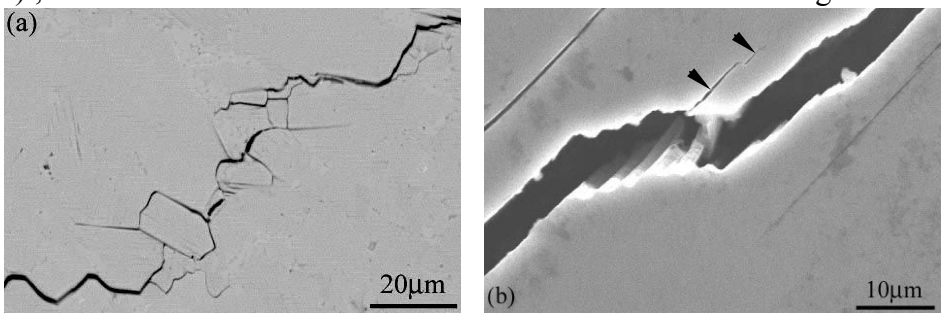

Fig.4 SEM micrographs of the crack path morphology

obscure. The slope of crack growth rate decreased slightly with increasing R. Modified Paris power-law relationship

$$da/dN = C (K_{max})^n(\Delta K)^p$$

is used which is often utilized to elucidate the fatigue mechanism of some structural ceramics. Here C, n and p are experimentally determined parameters. The exponent p is 3.4 from constant K_{max} with decreasing-K_{min} experiments. These behaviors indicate a strong dependence of the crack growth rate on K_{max} and weak dependence on ΔK.

C. Fatigue crack path observations

A clear intergranular fracture mode and intact grain bridging in the wake of crack tip can be seen in Fig. 4. Shear-induced microfaults are clearly observed in an individual grain, as shown by arrows in Fig. 4b, which can reduce the frictional pullout stress at the grain/matrix interface under cyclic fatigue, indicating additional energy dissipation due to friction. All these observations reflect the operation of multiple energy dissipative mechanisms [5], which render Ti_3SiC_2 to exhibit a higher threshold stress intensity and a lower crack growth rate.

3.2 Damage under cyclic Hertzian contact

A. Damage observation of indented surface

The evolution of top surface and subsurface damage under cyclic loading using bonded-interface specimen for Ti_3SiC_2 is shown in Fig. 5. At 10^6 cycles, bands of shear-faults and microfracture were well developed. Wear debris are observed in such damage zones. Similar to other ceramics at Hertzian contact [6,7], the debris in Hertzian damage zone originated from frictional attrition at weak interface by shear stress in compression-shear contact field. Energy dispersives X-ray of such debris indicates that oxidation happened during friction between the weak interfaces. Radial cracks were observed at higher cycles, as shown in Fig. 5 (c). For Hertzian contact in Ti_3SiC_2, the

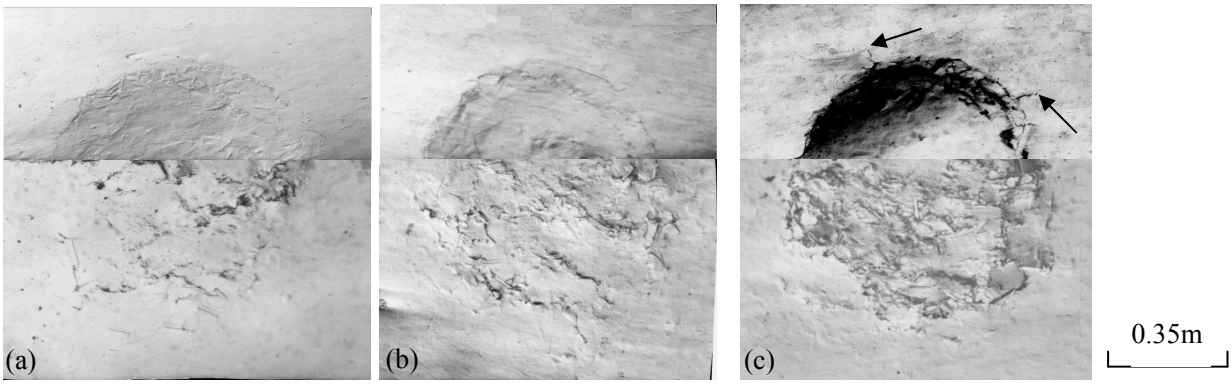

Fig. 5 Optical micrographs in Nomarski illumination, showing surface (top) and subsurface (bottom) damage in Ti_3SiC_2 at peak load 1000 N and different cycles. (a) 10^0, (b) 10^3, (c) 10^6

underlying damage mechanism of such higher wear rates is frictional wear at weak interface, which is similar to that under conventional long crack tensile tests.

B. Strength degradation

Fig. 6 plotted the flexural strength of Ti_3SiC_2 specimens subjected to cyclic Hertzian contacts at load range 0 ~ 1000N. Hatched box near the strength axis represents unindented specimens. Ti_3SiC_2 shows a gradual fall off in strength with the number of cycles even though strength degradation is measured after one cycling. This is similar to the trend of strength degradation observed in heterogeneous brittle solids [8,9], reflecting damage tolerance of such heterogeneous structural materials. It is noticed that radial cracks form at higher number of cycles, as shown by arrows in Fig. 5 (c). The formation of radial crack may induce further strength degradation.

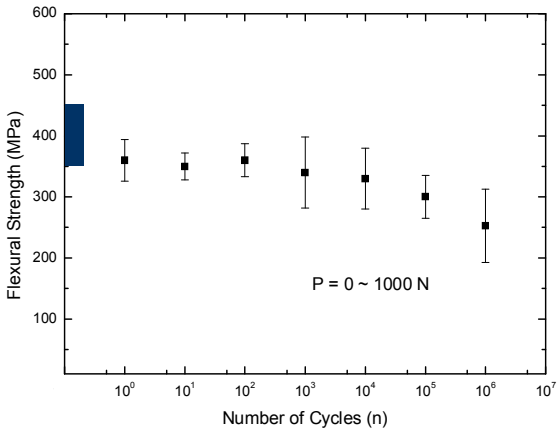

Fig. 6 Flexural strength of Ti_3SiC_2 specimen as a function of number of contact cycles.

The degree of strength degradation in Ti_3SiC_2 is lower than some heterogeneous ceramics in the same selected cyclic range [7,8]. Microstructural observations revealed that the intensity of the subsurface damage increased steadily with the number of cycles, whereas the size of damage zone remains nearly unchanged. No obvious bands of grain dislodgment are observed even at 10^6 cycles. From the results of strength degradation, it is deduced that radial cracks are more deleterious than material removal in the subsurface damage zone.

Summary

Ti_3SiC_2 exhibits exceptional “small crack” behavior and a relatively higher threshold stress intensity and lower crack growth rate. Damage zone formed in subsurface of specimen at Hertzian contact. The damage developed with the number of cycles, indicating a mechanical effect. Strength degradation from Hertzian contact is steady. Mechanisms underlying fatigue behavior is frictional wear at weak interfaces.

Acknowledgments: This work was subsidized with the Special Funds for the major State Basic Research Projects under No. 19990650.

References

[1] M.W. Barsoum and T. EI-Raghy, J. Am. Ceram. Soc., 79 (1996) 1953.
[2] Z.F. Zhang, Z.M. Sun and H. Hashimoto, Metall. Mater. Trans., 33A (2002) 3321.
[3] Z.M. Sun, Z.F. Zhang, H. Hashimoto and T. Abe, Mater. Trans., 43 (2002) 432.
[4] H. Cai, M.A.S. Kalceff and B.R. Lawn, J. Mater. Res., 9 (1994) 762.
[5] C.J. Gilbert, D.R. Bloyer, M.W. Barsoum, A.P. Tomsia and R.O. Ritchie. Scripta Mater., 42 (2000) 761.
[6] N.P. Padture and B.R. Lawn, Acta Mater., 43 (1995)1609.
[7] N.P. Padture and B.R. Lawn, J. Am. Ceram. Soc., 78 (1995) 1431.
[8] F. Guiberteau, N.P. Padture, H. Cai and B.R. Lawn, Philo. Mag. A, 68 (1993) 1003.
[9] H. Cai, M.A.S. Kalceff, B.M. Hooks and B.R. Lawn, J. Mater. Res., 9 (1994) 2654.